

Radiation loss of coupled-resonator waveguides in photonic-crystal slabs

M. L. Povinelli^{a)} and Shanhui Fan

Ginzton Laboratory, Stanford University, Stanford, California 94305

and Department of Electrical Engineering, Stanford University, Stanford, California 94305

(Received 29 August 2006; accepted 30 September 2006; published online 8 November 2006)

The authors characterize the intrinsic radiation loss of coupled-resonator optical waveguides by defining a waveguide-quality factor Q . They find that tuning an isolated resonator in a photonic-crystal slab to maximize its Q can also increase the waveguide Q . Due to interference between different resonators, the waveguide can have far lower loss than the isolated cavity; in other cases it can have far greater loss. They show that the dependence of waveguide Q on wave vector can largely be predicted by the shifting of the light cone within a tight-binding model. © 2006 American Institute of Physics. [DOI: 10.1063/1.2387131]

Coupled-resonator optical waveguides (CROWs),^{1,2} in which light “hops” between localized resonator modes, allow the significant reduction of light speed on chip. In dynamically tuned CROWs, light may even be stopped and stored³ to create dispersion-free time delays,⁴ useful for optical communications applications such as true-time delay, buffering, and the resolution of packet contention. Several groups have experimentally demonstrated CROWs within photonic-crystal slabs,^{5–10} but with relatively high waveguide loss. Loss can arise from disorder such as slight variations in individual resonators,¹¹ as well as poor input coupling to the CROW mode; the latter can be minimized using adiabatic tapering schemes.¹² More fundamentally, however, in a photonic-crystal slab, even a perfect CROW without any disorder suffers from *intrinsic* radiation loss, in which the CROW mode leaks vertically out of the slab as it propagates. Very little quantitative work has been done to determine the value of the radiation loss or elucidate its dependence on the waveguide parameters. Meanwhile, recent work has shown tremendous progress in reducing the vertical radiation loss of *single*, isolated resonators in a photonic-crystal slab.^{13–15} A natural question to ask is whether such improved single-resonator designs can be adapted to produce low-loss CROW waveguides. Here we show that optimizing the design of a single resonator can also greatly reduce the losses of CROW waveguides. Moreover, we find that in certain cases, the radiation loss of the CROW waveguide can actually be *far lower* than for an isolated cavity. We further adapt the light-cone formulation of cavity quality factor Q (Ref. 16) to the case of propagating modes and show how it can predict the general trends observed in our numerical simulations.

We consider the structure shown in Fig. 1(a). The bulk photonic crystal is a triangular lattice of air holes with lattice constant a and hole radius $r=0.29a$ in a suspended, dielectric slab with height $0.6a$ and refractive index $n=3.45$ (silicon). The CROW waveguide is formed by periodically spaced defects (resonators) with a center-to-center separation of L ($6a$ in figure). Each defect is formed by removing three holes along the x direction and shifting the nearest neighbor holes on either side outward by an amount s [Fig. 1(b)]. The isolated defect has previously been shown to have a very high cavity quality factor $Q \approx 50\,000$ for $s=0.15a$.^{17,18}

We calculated the dispersion relation and loss of the CROW waveguide for periodicities $L=5a$, $6a$, and $7a$ using

three-dimensional finite-difference time domain (FDTD) simulations^{19,20} with a resolution of 20 grid points per a . The computational cell was set to be Bloch periodic in the x direction with fixed wave vector k . To measure the intrinsic, vertical radiation loss from the slab, we set the length of the cell in the y direction large enough ($=16\sqrt{3}a$) for the loss to be independent of length and applied periodic boundary conditions. Perfectly matched layer absorbing boundaries were used in the vertical (z) direction. The intersection of the computational unit cell with the $L=6a$ structure is shown by the thick solid line (orange online) in Fig. 1(a).

For each of the structures, the dispersion relation of the CROW band lies close to the frequency of the isolated cavity ($\omega=0.266[2\pi c/a]$). The center frequency, bandwidth, and sign of the slope of the band are summarized in Table I. The light line is given by $\omega_{ll}=ck$. At the edge of the Brillouin zone, the Bloch wave vector $k=0.5[2\pi/L]$ and $\omega_{ll}=0.5[2\pi c/L]=0.5(a/L)[2\pi c/a]$, which equals 0.1, 0.083, and 0.07 $[2\pi c/a]$ for $L=5a$, $6a$, and $7a$, respectively. In all cases, the CROW mode is intrinsically lossy because the CROW band lies above the light line.

In order to compare the loss of the CROW waveguide to the loss of an isolated cavity, we define a waveguide-quality factor $Q(k)$. In analogy to cavities, $Q(k)$ is equal to $\omega(k)$ times the $1/e$ power-decay time of the waveguide mode.

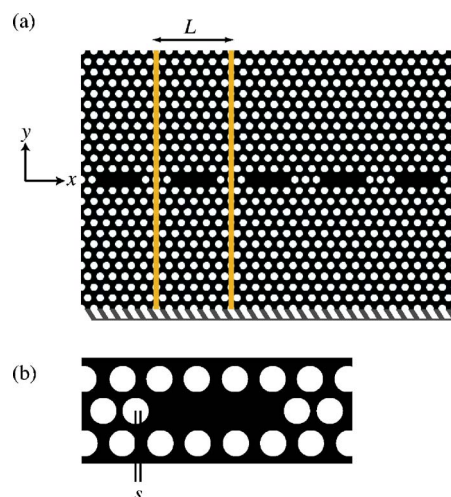


FIG. 1. (Color online) (a) Coupled-resonator waveguide in a photonic-crystal slab. (b) Magnified view of the resonator, showing outward hole shift s .

^{a)}Electronic mail: mpovinel@stanford.edu

TABLE I. CROW band parameters.

L	$s=0a$			$s=0.15a$		
	$\omega_o[2\pi c/a]$	$\Delta\omega/\omega_o$	$v_g(k>0)$	$\omega_o[2\pi c/a]$	$\Delta\omega/\omega_o$	$v_g(k>0)$
5a	0.268	0.004	≥ 0	0.267	$5E-4$	≥ 0
6a	0.268	$5E-4$	≤ 0	0.266	0.001	≤ 0
7a	0.268	$8E-4$	≤ 0	0.266	$6E-4$	≤ 0

$Q(k)$ can be converted to a k -dependent $1/e$ power-decay length in the waveguide as $L_{1/e}(k) = v_g(k)Q(k)/\omega(k)$ or to loss in dB/length as $-4.34 \text{ dB}/L_{1/e}$. $Q(k)$ is well defined over the entire Brillouin zone, while the loss per unit length diverges at $k=0$ and $0.5[2\pi/L]$, where the group velocity goes to zero. We calculated $Q(k)$ directly with a standard FDTD method, using a narrow band, pulsed source to excite the mode of interest and extracting the decay time from the field magnitude after source turnoff.²¹

Results for $Q(k)$ are shown in Fig. 2. Results of the direct calculation are shown by solid lines ($s=0a$) and dashed lines ($s=0.15a$). Black arrows indicate the Q of the isolated cavity for $s=0a$ and gray (red online) arrows for $s=0.15a$. For the unshifted-hole case ($s=0a$), the CROW Q lies below the Q of the isolated cavity for all periodicities. However, for the shifted-hole case ($s=0.15a$), the CROW Q lies at least partially above the isolated-cavity Q . This trend is most pronounced for $L=6a$ [Fig. 2(b)], where the CROW $Q \approx 370\,000$ at $k=0$, an order of magnitude higher than the isolated-cavity value. The fact that the CROW Q can be either higher or lower than the Q of an isolated cavity indicates that interference between the cavities strongly affects the radiation leakage. Interestingly, the trends in $Q(k)$ are not

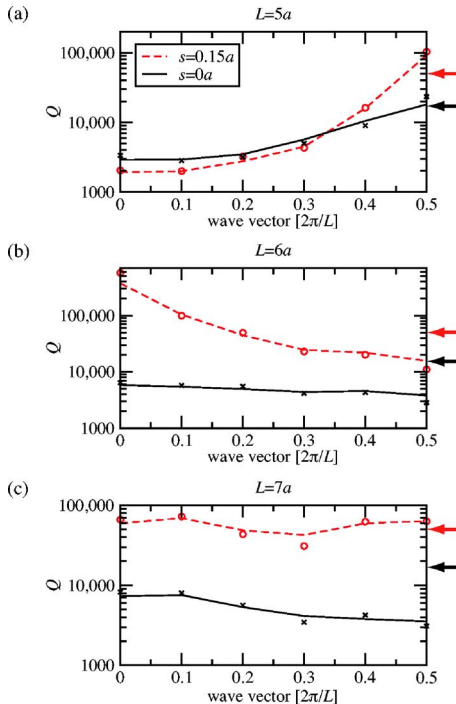


FIG. 2. (Color online) $Q(k)$ for various CROW periodicities L . Lines are results of direct calculation method; symbols are results of light-cone integration method. Arrows indicate the Q of the isolated resonators with $s=0.15a$ (gray/red online) and $s=0a$ (black). (a) $L=5a$, (b) $L=6a$, and (c) $L=7a$.

universal; Q increases with k for $L=5a$ [Fig. 2(a)] and $L=6a$ [Fig. 2(b)], while Q tends to decrease with k for $L=7a$ [Fig. 2(c)] and $s=0a$ (the $s=0.15a$ curve initially decreases and then rises in a “notch” shape). Below, we provide an explanation for these trends.

For isolated microcavities, it has been shown that Q can be related to the Fourier transform of the electromagnetic fields above the surface of the slab.^{16,22} Here we extend the analysis to $Q(k)$ for periodic waveguides. We start by expressing

$$Q(k) = \omega(k) \frac{\langle u(k) \rangle}{\langle p(k) \rangle}, \quad (1)$$

where ω is the frequency of the mode at wave vector k , $\langle u(k) \rangle$ is the time-averaged electromagnetic field energy per unit cell,

$$\langle u(k) \rangle \equiv \frac{1}{2} \int dv (\epsilon E_k^2(x, y, z) + \mu H_k^2(x, y, z)), \quad (2)$$

and $\langle p(k) \rangle$ is the time-averaged emitted power per unit cell. All time averages are over one optical cycle. To find $\langle p(k) \rangle$, we first consider the total power $\langle P(k) \rangle$ emitted from an infinitely long CROW waveguide, which can be written in terms of the two-dimensional (2D) spatial Fourier transforms of the free-space fields on any surface above the structure:¹⁶

$$\begin{aligned} \langle P(k) \rangle = & \frac{\sqrt{\mu_o/\epsilon_o}}{2} \int_{q_{\parallel} \leq \omega(k)/c} \frac{dq_x dq_y}{2\pi 2\pi} \left(\frac{\epsilon_o}{\mu_o} |\tilde{E}_{k,x}(q_x, q_y)|^2 \right. \\ & + \frac{\epsilon_o}{\mu_o} |\tilde{E}_{k,y}(q_x, q_y)|^2 + |\tilde{H}_{k,x}(q_x, q_y)|^2 \\ & \left. + |\tilde{H}_{k,y}(q_x, q_y)|^2 \right), \quad (3) \end{aligned}$$

where $q_{\parallel} = (q_x^2 + q_y^2)^{1/2}$. $\tilde{E}_{k,x}$ denotes the 2D Fourier transform of the x component of \mathbf{E}_k (denoted as $E_{k,x}$), defined as

$$\tilde{E}_{k,x}(q_x, q_y) \equiv \int dx \int dy E_{k,x}(x, y) e^{iq_x x + iq_y y},$$

and similarly for other components. The Fourier-space integral includes only q_{\parallel} components lying above the light line, for these are the components that contribute to the radiation loss. From Bloch's theorem, the fields can be rewritten as $\mathbf{E}_k(x, y, z) = e^{ikx} \mathcal{E}_k(x, y, z)$ and $\mathbf{H}_k(x, y, z) = e^{ikx} \mathcal{H}_k(x, y, z)$, where \mathcal{E}_k and \mathcal{H}_k are periodic in the unit cell. It follows that the emitted power per unit cell can be written as

$$\begin{aligned} \langle p(k) \rangle = & \frac{\sqrt{\mu_o/\epsilon_o}}{2} \int_{q_{\parallel} \leq \omega(k)/c} \frac{dq_x dq_y}{2\pi 2\pi} \left(\frac{\epsilon_o}{\mu_o} |\tilde{\mathcal{E}}_{k,x}(q_x + k, q_y)|^2 \right. \\ & + \frac{\epsilon_o}{\mu_o} |\tilde{\mathcal{E}}_{k,y}(q_x + k, q_y)|^2 + |\tilde{\mathcal{H}}_{k,x}(q_x + k, q_y)|^2 \\ & \left. + |\tilde{\mathcal{H}}_{k,y}(q_x + k, q_y)|^2 \right), \quad (4) \end{aligned}$$

where the integral in the 2D Fourier transform is taken over one unit cell.

We explicitly verified the validity of the light-cone formulation by calculating $Q(k)$ from Eqs. (1), (2), and (4). The periodic part of the fields was extracted from the full field obtained in the FDTD simulation by dividing by the known

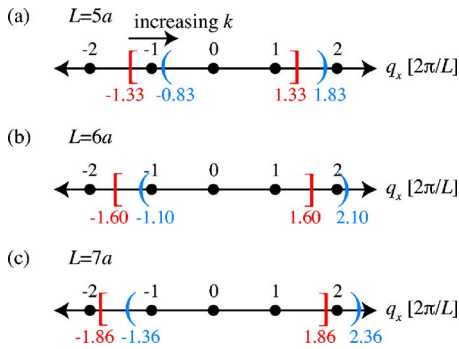


FIG. 3. (Color online) Number of Fourier components inside the light cone. (a) $L=5a$, (b) $L=6a$, and (c) $L=7a$.

Bloch phase. In the x direction, the Fourier spectrum is discrete with spacing $2\pi/L$, where L is the CROW periodicity. In the y direction, the spacing is determined by the length of the supercell and approximates a continuous distribution for large enough supercell size. The 2D discrete Fourier transform was taken on a plane $0.2a$ above the top surface of the slab. We have verified that the result is independent of height outside the slab. The results are shown as symbols in Figs. 2(a)–2(c). Agreement with the direct calculation method is good and clearly predicts the dependence of Q on k . We attribute the discrepancies in the data to numerical error due to the small number of discrete Fourier components inside the light line.

Interestingly, we can predict the trend in $Q(k)$ quite simply if we assume that the fields are well described by the tight-binding approximation.¹ In this approximation, $\mathcal{E}_k(x, y, z) \approx \mathcal{E}(x, y, z)$, independent of k . Making a change of variables in Eq. (4), $\langle p(k) \rangle$ is given by the integral of a k -independent function over a shifted light cone:

$$\begin{aligned} \langle p(k) \rangle &= \frac{\sqrt{\mu_o \epsilon_o}}{2} \int_{\sqrt{(q_x - k)^2 + q_y^2} \leq \omega(k)/c} \frac{dq_x dq_y}{2\pi \cdot 2\pi} \\ &\times \left(\frac{\epsilon_o}{\mu_o} |\tilde{\mathcal{E}}_x(q_x, q_y)|^2 + \frac{\epsilon_o}{\mu_o} |\tilde{\mathcal{E}}_y(q_x, q_y)|^2 \right. \\ &\left. + |\tilde{\mathcal{H}}_x(q_x, q_y)|^2 + |\tilde{\mathcal{H}}_y(q_x, q_y)|^2 \right). \end{aligned} \quad (5)$$

The wave vector components lying inside the light line are shown in Fig. 3. For simplicity, we draw the intersection of the light cone with the $q_y=0$ axis. The spacing of the discrete Fourier components q_x is $2\pi/L$, indicated by the black dots. The frequency of the CROW band is fixed at $\omega \approx 0.266[2\pi c/a]$. The position of the light cone for $k=0$ is indicated by the square brackets and is found from $|q_x| < \omega/c \approx 0.266[2\pi/a] = 0.266(L/a)[2\pi/L]$. As L increases, the light cone becomes larger. As k increases, the light cone shifts to the right. The position of the light cone for $k=0.5[2\pi/L]$, the edge of the Brillouin zone, is shown by round brackets. For $L=5a$ [Fig. 3(a)], the number of discrete Fourier components above the light line decreases from 3 to 2 with increasing k . Fewer Fourier components correspond to less power leakage and increasing $Q(k)$, correctly predicting the trend in Fig. 2(a). For $L=6a$ [Fig. 3(b)], the number of discrete Fourier components increases from 3 to 4, corresponding to increasing loss and decreasing $Q(k)$, also in agreement with the observed results of Fig. 2(b). For $L=7a$ [Fig. 3(c)], the Fourier picture also predicts decreasing $Q(k)$,

in accordance with the $s=0$ results in Fig. 2(c). However, it can not predict the details of the notched shape seen in Fig. 2(c) for $s=0.15a$, which results from slight deviations of the fields from the tight-binding form and redistribution of the power spectrum. For the tight-binding model to be valid, the evanescent coupling of neighboring defects through the crystal must dominate over any radiative coupling in the air. For this reason, it is not entirely surprising that the tight-binding prediction begins to fail at increasing periodicities, where the evanescent coupling is expected to be weakest.

The results of this letter suggest that the waveguide Q of a CROW waveguide can be far higher or lower than that of the cavities of which it is composed. Moreover, the dependence of Q on wave vector can be dramatic, spanning more than an order of magnitude across the waveguide band, and varies strongly with CROW periodicity. These considerations should be taken into account in any future CROW designs. The validity of the light-cone method for calculating CROW waveguide losses should also allow further optimization of such structures, such as by inverse-design techniques.²²

The authors thank Ilya Fushman and Jelena Vučković for helpful discussions of the light-cone method. This work was funded by a L'ORÉAL USA Fellowship for Women in Science, the DARPA Slow Light Program (Grant No. FA9550-05-0414), and the Packard Foundation.

- ¹A. Yariv, Y. Xu, R. K. Lee, and A. Scherer, *Opt. Lett.* **24**, 11 (1999).
- ²N. Stefanou and A. Modinos, *Phys. Rev. B* **57**, 12127 (1997).
- ³Mehmet F. Yanik, and Shanhui Fan, *Phys. Rev. Lett.* **92**, 083901 (2004).
- ⁴Sunil Sandhu, M. L. Povinelli, M. F. Yanik, and Shanhui Fan, *Opt. Lett.* **31**, 1985 (2006).
- ⁵S. Olivier, C. Smith, M. Rattier, H. Benisty, C. Weisbuch, T. Krauss, R. Houdré, and U. Oesterlé, *Opt. Lett.* **26**, 1019 (2001).
- ⁶E. Ozbay, M. Bayindir, I. Bulu, and E. Cubukcu, *IEEE J. Quantum Electron.* **38**, 837 (2002).
- ⁷T. J. Karle, D. H. Brown, R. Wilson, M. Steer, and T. F. Krauss, *IEEE J. Quantum Electron.* **8**, 909 (2002).
- ⁸T. D. Happ, M. Kamp, A. Forchel, J.-L. Gentner, and L. Goldstein, *Appl. Phys. Lett.* **82**, 4 (2003).
- ⁹A. D. Bristow, D. M. Whittaker, V. N. Astratov, M. S. Skolnick, A. Tahaoui, T. F. Krauss, M. Hopkinson, M. P. Croucher, and G. A. Gehring, *Phys. Rev. B* **68**, 033303 (2003).
- ¹⁰P. Sanchis, J. Martí, W. Bogaerts, P. Dummon, D. Van Thourhout, and R. Baets, *IEEE Photonics Technol. Lett.* **17**, 1199 (2005).
- ¹¹B. Z. Steinberg, A. Boag, and R. Lisitsin, *J. Opt. Soc. Am. A* **20**, 138 (2003).
- ¹²P. Sanchis, J. Garcia, A. Martinez, F. Cuesta, A. Griol, and J. Martí, *Opt. Lett.* **28**, 1903 (2003).
- ¹³Y. Akahane, T. Asano, B.-S. Song, and S. Noda, *Opt. Express* **13**, 1202 (2005).
- ¹⁴Bong-Shik Song, Susumu Noda, Takashi Asano, and Yoshihiro Akahane, *Nat. Mater.* **4**, 207 (2005).
- ¹⁵Eiichi Kuramochi, Masaya Notomi, Satoshi Mitsugi, Akihiko Shinya, and Takasumi Tanabe, *Appl. Phys. Lett.* **88**, 041112 (2006).
- ¹⁶J. Vučković, M. Lončar, H. Mabuchi, and A. Scherer, *IEEE J. Quantum Electron.* **38**, 850 (2002).
- ¹⁷Y. Akahane, T. Asano, B.-S. Song, and S. Noda, *Nature (London)* **425**, 944 (2003).
- ¹⁸Ziyang Zhang and Min Qiu, *Opt. Lett.* **30**, 1713 (2005).
- ¹⁹D. Roundy, M. Ibanescu, P. Bermel, A. Farjadpour, J. D. Joannopoulos, and S. G. Johnson, MEEP FDTD package, 2006, <http://ab-initio.mit.edu/meep>
- ²⁰Karl S. Kunz and Raymond J. Luebbers, *The Finite-Difference Time-Domain Method for Electromagnetics* (CRC, Boca Raton, FL, 1993).
- ²¹Vladimir A. Mandelshtam, and Howard S. Taylor, *J. Chem. Phys.* **107**, 6756 (1997).
- ²²Dirk Englund, Ilya Fushman, and Jelena Vučković, *Opt. Express* **13**, 5961 (2005).